ARTICLES

XPS and UPS Characterization of the TiO_2/ZnPcGly Heterointerface: Alignment of Energy Levels

Guangming Liu* and W. Jaegermann

Department of Material Science, Darmstadt University of Technology, Petersenstrasse 23, D-64287 Darmstadt, Germany

Jianjun He and Villy Sundström

Department of Chemical Physics, Lund University, S-221 00 Lund, Sweden

Licheng Sun

Department of Organic Chemistry, Stockholm University, S-106 91 Stockholm, Sweden

Received: November 14, 2001; In Final Form: March 19, 2002

The electronic structure and the highest occupied molecular orbitals (HOMO)/the lowest unoccupied molecular orbitals (LUMO) alignment at the molecular semiconductor heterointerface of nanostructured TiO_2/ZnPcGly dye sensitizer were characterized by X-ray and ultraviolet photoemission spectroscopy (XPS and UPS). The HOMO level of the dye ZnPcGly was determined to be located at 1.62 eV below the Fermi edge, and the corresponding LUMO level was estimated to be 0.10 eV above the conduction band of TiO_2 based on the HOMO/LUMO gap (1.82 eV) of ZnPcGly determined by optical absorption measurements. This energy level matching between the orbitals of the dye and the bands of TiO_2 can enable efficient electron transfer from photoexcited ZnPcGly to TiO_2, which is very important in photoinduced charge-transfer reactions and for applications in dye-sensitized solar cells.

Introduction

The dye sensitized thin film solar cell (DSSC) has attracted much interest for application in solar energy conversion since Grätzel et al. first reported a high overall solar-to-electric conversion efficiency of ∼10%.[1] Various phthalocyanine dyes are promising and attractive materials for dye-sensitized nanostructured solar cells because they possess intensive absorption in the far red/near-IR spectral region and have appropriate redox properties for the sensitization of large band gap semiconductors (TiO_2).[2] In addition, they exhibit excellent chemical, thermal and light stability. Phthalocyanine photoelectrochemistry has also shown improvement in energy conversion efficiency over the past decades.[3] The conversion efficiency mainly depends on energy matching (HOMO/LUMO) between the dye and the semiconductor and the dye and the redox couple, charge separation and recombination, and fast electron transfer between the sensitizing dye and the semiconductor. Theoretically, the dye's LUMO after photoexcitation is above the semiconductor conduction band (CB) edge (i.e., closer to vacuum energy level), and the $E_{LUMO} - E_{CB}$ difference presents an enthalpic driving force at the interface for charge separation and electron injection.[4] The injection rate of the electron into the conduction band will depend on the level matching of the excited state of the molecule with the conduction band states. In addition, the charge-transfer process is also sensitive to the electronic structure at the interface, since interface states may act as recombination centers for excited charge carriers and produce loss processes in solar cells.

The relative positions of energy levels at the dye/semiconductor interface were usually estimated from different optical and electrochemical measurements,[5] photoelectric threshold measurements,[6] and even by means of X-ray photoelectron spectroscopy[7] and surface photovoltage spectroscopy techniques, etc.[8] However, very few ultrahigh vacuum (UHV) investigations on the electronic structure of the semiconductor TiO_2/dye heterointerface have appeared in the literature,[7] which is still not well understood in its microscopic details. It is therefore of high interest to study the nature of this heterointerface, and to determine the alignment between HOMO and LUMO states of the dye adsorbed on the semiconductor (TiO_2) surface. In addition, insight into the electronic band structure of this molecular semiconductor interface is also useful to predict, understand and further optimize the photoelectrical properties and performance of photovoltaic systems. Surface analysis studies by combined X-ray photoemission spectroscopy (XPS) and ultraviolet photoemission spectroscopy (UPS) can be used to investigate the electronic structure, the valence band, core levels of related components, and the relative positions of the energy levels involved in the interface of semiconductor TiO_2/sensitizing dye.

* Corresponding author. Tel.: +49-6151-166354. Fax: +49-6151-166308. Email: gmliu@surface.tu-darmstadt.de.

10.1021/jp014192b CCC: $22.00
Published on Web 05/15/2002

Based in part on our earlier work, where we have successfully determined the band alignment at various inorganic semiconductor heterojunctions by a combination of UPS and XPS measurements during a multistep growth sequence of thin film solar cells,[9] we present here our first results on the use of combining XPS and UPS for the determination of HOMO and LUMO states alignment at the interface between nanostructured TiO_2 and 2,9,16,23-tetra(carbonylmethylaminocarboxyl) phthalocyaninato zinc(II) (ZnPcGly) dye (see molecular structure below) under UHV conditions. The highest monochromatic incident photon-to-current conversion efficiency (IPCE) of 5.5% at 690 nm and an overall conversion efficiency of 0.13% were achieved for a sandwich solar cell based on a ZnPcGly sensitized TiO_2 electrode.[10]

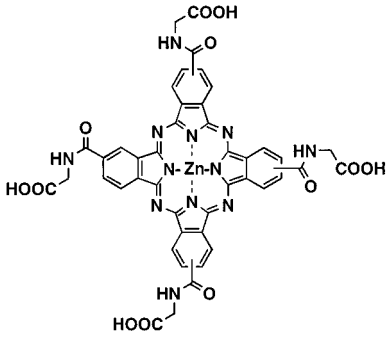

Molecular Structure of Dye (ZnPcGly)

Experimental Section

Photoelectron Spectroscopy. The experiments were carried out in an integrated ultrahigh vacuum (UHV) system equipped with multitechnique surface analysis system (Physical Electronics 5700) photoelectron spectrometer (XPS and UPS) and connected with a electrochemical chamber, a preparation chamber, a molecular beam epitaxy (MBE) chamber, and an oxide growth chamber, allowing in situ characterization of the prepared films and surfaces (base pressure 1×10^{-10} Torr). An Ar ion gun is available for in situ cleaning of the substrate surface. The XP spectra of the samples were measured with monochromatized Al Kα radiation. The scale of the binding energy (BE) was calibrated against Au($4f_{7/2}$). UPS were measured with a negative bias voltage (-1.55 V) applied to the samples using the He(I) (21.2 eV) and He(II) (40.8 eV) line in order to shift the spectra from the spectrometer threshold. The spectra were calibrated vs the Fermi edge of polycrystalline Au.

Preparation of TiO_2 Film. Colloidal TiO_2 solution (Ti$-$Nanoxide T) with solid particle size at ca. 13 nm was purchased from Solaronix S. A., Switzerland. Nanostructured TiO_2 films were prepared on a transparent conducting oxide (TCO) glass substrate (F doped SnO_2; sheet resistance $10-15\ \Omega/\square$), using Scotch tape as a spacer, by distribution of the colloidal TiO_2 solution and raking off the excess suspension with a glass rod. The films were dried and then heated at 450 °C for 1 h in air. The thickness of the TiO_2 films is 2.6 μm, measured by a Dektak 3 surface profile measuring system.

Dye Coating. Adsorption of the dye was performed by dipping the TiO_2 substrate for at least 3 h into a 5×10^{-5} M solution of the dye (ZnPcGly) in dry ethanol containing 3% of dimethyl sulfoxide (DMSO, v/v). This dye-coating was performed at a substrate temperature of ca. 80 °C immediately after the high-temperature annealing of the TiO_2 film in order to avoid hydration of the TiO_2 surface or capillary condensation of water vapor from ambient air inside the nanoporous of the film. After completion of dye adsorption, the sample was withdrawn from the solution, rinsed with dry ethanol several times, and dried with a stream of dry N_2 of high purity. This procedure is expected to yield monolayer coverage of the dye on the TiO_2 film surface,[11,12] with possibility of some surface aggregation. Then the sample was immediately transferred into the UHV chamber for measurements.

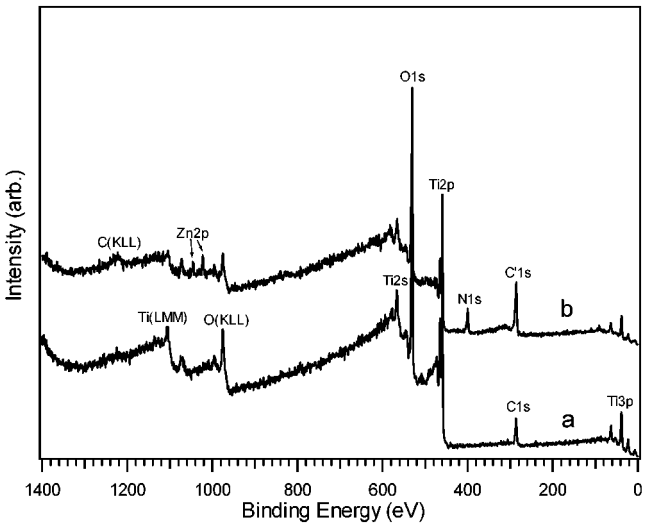

Figure 1. X-ray photoelectron spectra of (a) TiO_2 film and (b) TiO_2/ZnPcGly interface deposited on transparent conducting oxide (TCO) glass.

Results and Discussion

Photoelectron spectroscopy (PES) was used to investigate the chemical composition and electronic structure of the TiO_2 (anatase) polycrystalline thin films. The stoichiometry and oxidation state of deposited films were analyzed based on the Ti 2p and O 1s core levels with an energy resolution of 0.4 eV.

XP spectra of the TiO_2 film after deposition onto the TCO glass substrate are shown in Figure 1 (spectrum a). The deposited film is mainly composed of Ti and O, except a small amount of C1s emission can be observed, which may result from the ex situ preparation process or the transfer process of the sample into the UHV chamber. The C contamination only occurs on the surface of the TiO_2 film, because the intensity of the C1s signal can dramatically be decreased with Ar ion sputtering and no C signal is detected after a very short time, which indicates that no C is incorporated into the TiO_2 film.

Figure 2 shows XPS core level spectra for the deposited TiO_2 film surface before and after Ar ion sputtering. The unsputtered surface exhibits two peaks of $Ti2p_{1/2}$ (465.1 eV) and $Ti2p_{3/2}$ (459.4 eV) in Figure 2a, which are assigned to Ti^{4+} oxidation state of the stoichiometric oxide TiO_2 according to reported XPS data.[13] The peak separation between the $2p_{1/2}$ and $2p_{3/2}$ lines is 5.7 eV, which is also consistent with $+4$ oxidation state.[14,15] After Ar ion sputtering (at a beam energy of 1 keV) the Ti2p spectra were broadened and the intensity was decreased, while some new emissions appeared at 457.5 and 455.6 eV and their intensities increased with sputtering time, indicating the formation of a small amount of reduced oxidation states of Ti^{3+} and Ti^{2+} species.[16,17] At this stage, the total Ti $2p_{3/2}$ spectra can be fitted by introducing two additional Ti^{3+} and Ti^{2+} $2p_{3/2}$ peaks at lower binding energies. The O1s spectra of the TiO_2 films in Figure 2b are asymmetric and show the contributions of three components: the main component is titanium dioxide (530.6

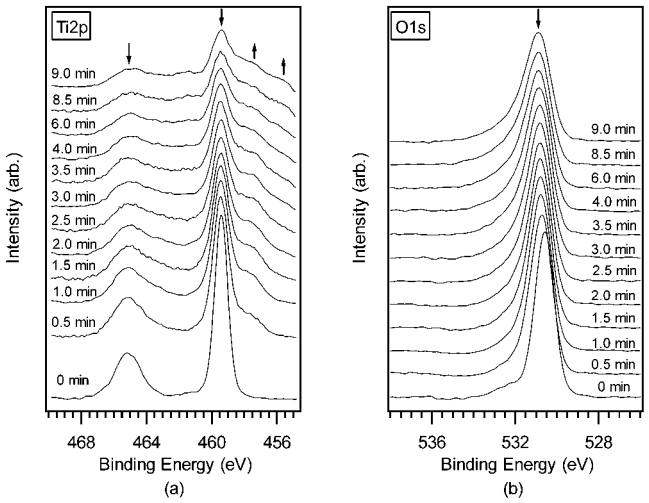

Figure 2. X-ray photoelectron spectra in the Ti2p region (a) and O1s region (b) for unsputtered and sputtered surface of TiO_2 film. Spectra from bottom to top correspond to cases where TiO_2 was unsputtered, after sputtering for 0.5, 1.0, 1.5, 2.0, 2.5, 3.0, 3.5, 4.0, 6.0, 8.5, and 9.0 min, respectively.

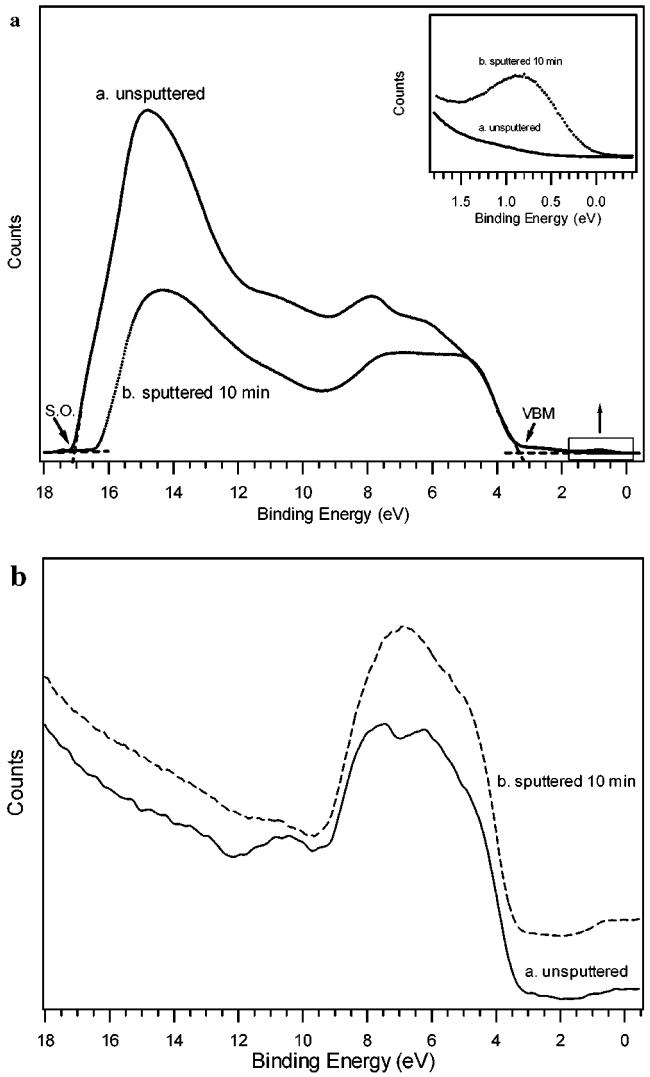

Figure 3. (a) Ultraviolet photoelectron spectra (He I) for the surface of unsputtered and sputtered TiO_2 films. (b) Ultraviolet photoelectron spectra (He II) for the surface of unsputtered and sputtered TiO_2 films.

eV); the other two smaller components may be hydroxyl groups or defective oxides (531.5 ± 0.5 eV), and adsorbed water (533 ± 1 eV),[15] which inevitably arise from the preparation and transfer process of the film. The O1s spectra also decreased in intensity and shifted to high binding energy along with the sputtering time. The surface defects (Ti^{3+} 3d defect states) play an important role in determining the electrochemical and photocatalytical properties of TiO_2. The importance of Ti^{3+} surface states in mediating interfacial charge-transfer processes at the TiO_2/solution boundary has recently been established by laser photolysis studies[18] and by the optical electrochemical method.[19] However, no reduced oxidation states of Ti^{3+} and Ti^{2+} species in the prepared films can be detected within the signal-to-noise ratio of our surface analysis system photoelectron spectrometer (XPS and UPS) based on the PES results of the symmetric Ti2p and O1s peaks in XPS spectra (Figure 2) and Ti3d defect free in UPS spectra below (Figure 3), unless exposure to Ar ion sputtering. This also indicates that the reduced Ti^{3+} concentration in the TiO_2 films as prepared must be very small (if they exist on the TiO_2 surface) and below the sensitivity of our instruments.

In Figure 3a UPS (He I) spectra of the TiO_2 surface before and after Ar ion sputtering are shown. According to the unsputtered spectrum a, the value of the valence band maximum (VBM) is located at ca. 3.28 eV below the Fermi level (E_B = 0 eV) determined by fitting a straight line into the leading edge. This value indicates considerable high n doping of the TiO_2 film, as the band gap for TiO_2 (anatase) is estimated to be 3.2−3.3 eV according to our previous results and reference values.[20] The secondary electron onset (SO) on the left side of the spectra is 17.1 eV. The work function of TiO_2 was calculated to be 4.1 eV by subtracting the secondary electron onset position of the He I UPS spectra from the excitation energy (21.2 eV). It is increased with sputtering time as also shown in Figure 3a (spectrum b). This 4.1 eV value obtained for the work function of the TiO_2 film is some different with the reported value 4.45 eV (if at the same doping level) based on contact potential difference measurements by Kelvin probe.[21] This difference may arise from the influence of surface state or surface contamination resulting from the ex situ preparation process of the TiO_2 film or caused by the different measurement methods. The valence band of anatase TiO_2 shows two peaks: a broad one centered at ca. 6 eV and a narrow one at ca. 8 eV, which correspond mainly to π (nonbonding) and σ (bonding) O2p orbitals, respectively.[15] In addition, the sputtered TiO_2 exhibits an additional peak in the range of 0−2 eV, which can be seen in more detail in the insert of Figure 3a. This is a contribution from the lower oxidation state of Ti^{3+} 3d at ca. 0.8 eV below E_F (assigned to surface states from surface defects of oxygen vacancies) caused by Ar ion bombardment, which is in agreement with the variation of XPS core levels as discussed above. Furthermore, similar results can also be found in UPS spectra (He II) of the same sample with the unsputtered and sputtered surfaces in Figure 3b.

XP spectra of the TiO_2 substrate after deposition of dye ZnPcGly are shown in Figure 1 (spectrum b). Some new peaks (C′1s, N1s, and Zn2p) obviously arising from the dye overlayer appeared compared to spectrum a of the bare TiO_2 substrate. Figure 4 shows XPS core level spectra of the TiO_2 substrate and the dye ZnPcGly overlayer. The Ti 2p and O 1s spectra of the TiO_2 film in Figure 4a,b (spectra a) decreased in intensity with the coverage of the dye. More strikingly, both spectra show a slight shift (ca. −0.10 eV) to lower BE with coverage (spectra b). Considering the fact that the individual particle size is too small (≪the Debye screening length of the material) to support a space charge layer for TiO_2 nanoparticles,[22] and that the band

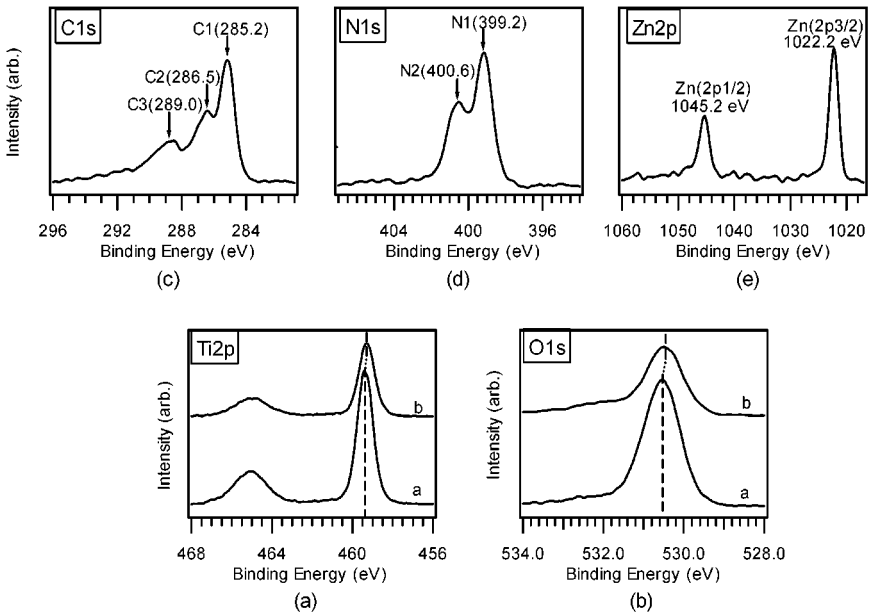

Figure 4. XPS core level spectra of the TiO_2 substrate and the dye (ZnPcGly) overlayer. (a,b) Ti 2p and O 1s level of TiO_2 film (spectra a) and TiO_2/ZnPcGly interface (spectra b); (c−e) C 1s, N 1s, and Zn 2p emission of the dye ZnPcGly.

bending across a nanocrystalline film is usually negligible, the core level binding energies shifts of the substrate TiO_2 semiconductor after coverage of the dye may be ascribed to charge redistribution in the interfacial region arising from the interaction (charge transfer or chemical interaction) between the semiconductor and the dye overlayer. Although spectrum b in Figure 4b is the total O1s spectrum from the dye and the TiO_2 substrate surface, the substrate signal is the dominating feature. The tailing of the emission line toward higher binding energies thus contains the signals due to carboxylic and carbonylic oxygens of the dye. Parts c−e of Figure 4 show the characteristic XPS core levels of C1s, N1s, and $Zn2p_{3/2}$ (1022.2 eV) lines of the dye ZnPcGly adsorbed on the TiO_2 film surface. The C1s in Figure 4c and N1s in Figure 4d XPS peaks obviously reflect the different chemical states of three carbon forms and two nitrogen forms in this dye molecule. Peak 1 (285.2 eV) of C1s results from aromatic carbons in the dye molecule overlayer and in a small part from the hydrocarbon contaminations adsorbed on the TiO_2 film as seen in Figure 1 (spectrum a); peak 2 (286.5 eV) originates from carbons bonded to N or O; and peak 3 (289.0 eV) with highest binding energy from carboxylic and carbonylic carbons of the dye molecule, which are consistent with the values as reported in the literature.[7,23] N1 (399.2 eV) and N2 (400.6 eV) are assigned to the contributions of nitrogen atoms in the aromatic ring and in the glycine substituents, respectively.[24]

The electronic energy levels of the ZnPcGly coated on the TiO_2 surface was estimated from UPS spectra (He I and He II). Figure 5a shows UPS spectra (He I) obtained from two different surfaces of TiO_2 and TiO_2/ZnPcGly before and after dye deposition, respectively. With the coverage of the dye, the TiO_2 spectra show more distinct photoemission peaks of the dye overlayer despite some superposition of the photoelectron emissions from the substrate layer. The insert of Figure 5a shows the HOMO emission region of the dye ZnPcGly in more detail. The bottom spectrum corresponds to the TiO_2 film layer on the TCO glass surface, which served as substrate for the formation of the junction between the organic dye and the semiconductor. The spectrum from the TiO_2/ZnPcGly surface exhibits an extra emission peak at 1.62 eV (see insert of Figure 5a). This peak can be attributed to photoelectrons from the highest occupied molecular orbital (HOMO) state of ZnPcGly adsorbed on TiO_2. This value is well consistent with the HOMO value of 1.60 eV for the same sample measured by He II spectra in Figure 5b. More intriguing in Figure 5a, there is a very small additional emission around 0.6 eV in UPS spectrum (He I) for the surface of TiO_2/ZnPcGly, which, however is not caused by the He I (β) satellite. Further evidence can also be found in He II spectrum of TiO_2/ZnPcGly (Figure 5b) and confirm that there is indeed existence of an emission (even increased in intensity due to the large surface sensitivity of He II), which is possibly caused by the substrate surface defect due to the charge transfer or chemical interaction between the substrate and the dye adsorbed on the surface. Additional experiments especially combination with band structure calculation are planned to further clarify this point. To determine the HOMO energy width, we need to remove the background emission from the substrate TiO_2 first to get a well defined HOMO peak shape in combination with peak fitting procedures. Then the HOMO maximum position at 1.62 eV can be decided by fitting a Gaussian line into the HOMO peak using Igor Pro software. The cutoff position was determined by fitting a straight line into the onset and determining the intersection point with the *x* axis. Thus the HOMO cutoff to maximum (HCM) value of 0.60 eV for the dye ZnPcGly was obtained by subtracting the cutoff position from the maximum position.

We estimate the LUMO positions for the dye overlayer by measuring the optical band gap value of the dye E_g(ZnPcGly) = 1.82 eV from a combination of optical and electrochemical measurements.[10] So the $LUMO_{max}$ energy level is obtained by subtracting the value of the band gap from the $HOMO_{max}$ value (note: the LUMO energy width cannot be determined from the XPS and UPS measurements):

$$E_{LUMO} = E_{HOMO} - E_g = 1.62\ \text{eV} - 1.82\ \text{eV} = -0.20\ \text{eV vs } E_F$$

Considering the small charge redistribution across the interface, the offset of the $LUMO_{max}$ value with E_{CB} of TiO_2 can be estimated:

$$E_{LUMOmax} - E_{CB}(TiO_2) = -0.10\ \text{eV}$$

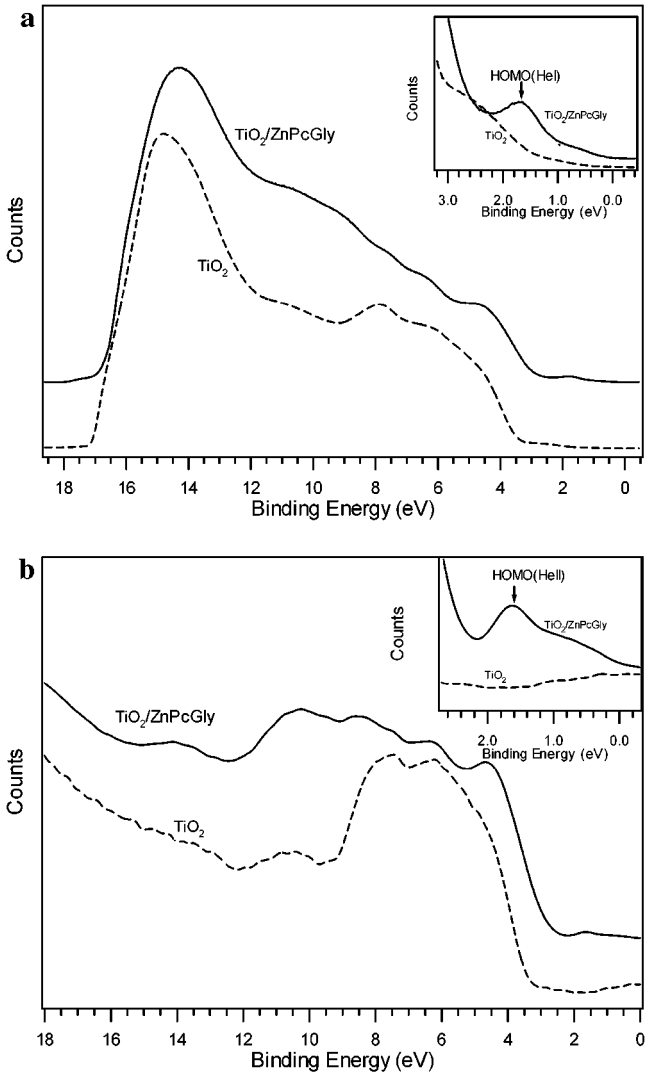

Figure 5. (a) Ultraviolet photoelectron spectra (He I) for surface of bare TiO_2 and TiO_2/ZnPcGly. Inset: UPS in the valence band region for TiO_2 and TiO_2/ZnPcGly. (b) Ultraviolet photoelectron spectra (He II) for surface of bare TiO_2 and TiO_2/ZnPcGly. Inset: UPS in the valence band region for TiO_2 and TiO_2/ZnPcGly.

When TiO_2 was coated with ZnPcGly, charge redistribution occurred due to the charge transfer or chemical interaction between the semiconductor and the dye overlayer. From these results, the $HOMO_{max}$ level of the dye ZnPcGly is determined to be located at 1.62 eV below E_F, i.e., 5.72 eV below the vacuum level (the TiO_2 work function is 4.10 eV as noted above, which corresponds to the energy distance of E_F to the vacuum level.); the $LUMO_{max}$ level is -0.20 eV above the E_F level, i.e., 3.90 eV below the vacuum level. These results on the alignment of energy levels of the TiO_2/ZnPcGly heterointerface are summarized in Figure 6 (0 V vs NHE is equivalent to -4.5 eV vs vacuum). The positions of the LUMO and HOMO peaks of the dye ZnPcGly fit well with the energy requirements for efficient electron injection into the conduction band of TiO_2 after light absorption.

Conclusions

In summary, the XPS core levels of TiO_2 anatase polycrystalline thin film and the dye ZnPcGly adsorbed on the semiconductor surface were used to investigate the stoichiometry and electronic structure of such interfaces by photoemission

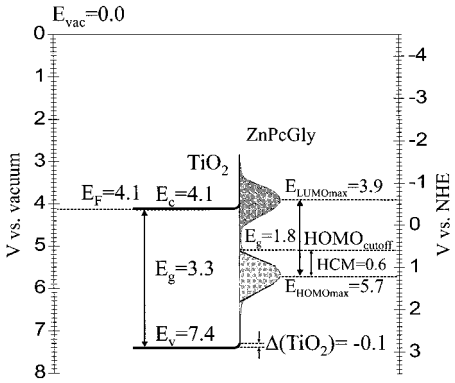

Figure 6. Energy diagram for nanoporous TiO_2 surface and TiO_2/ZnPcGly interface determined from XPS and UPS measurements.

spectroscopy. The position of the LUMO peak of the dye ZnPcGly (0.10 eV above E_{CB}) fits well with the energy requirements for efficient electron injection into the conduction band of TiO_2 semiconductor from the excited state of the molecule after light absorption. However, besides the high electron injection rate, conversion efficiency also depends on the charge recombination between the injected electron and the oxidized dye, and the redox potential matching between the dye and the redox couple in the electrolyte. Comparing with the ruthenium-polypyridine/TiO_2 system one of the most efficient dye sensitized solar cell, the relative low photovoltaic performance of ZnPcGly/TiO_2 sensitized solar cell should be caused by fast charge recombination (or $ZnPcGly^+$ reaction with I^-) while not by the electron injection as demonstrated by the reasonable alignment of TiO_2 band edge states and dye HOMO/LUMO levels evaluated from combined photoelectron spectroscopic measurements (XPS and UPS). In our future experiments, we plan to address the influence of solvent effects on the energy levels alignment by comparing UHV experiments using coadsorbed electrolyte with the results obtained by in situ experiments.

Acknowledgment. We acknowledge financial support of this work by the Alexander von Humboldt Foundation in Germany. We thank Dr. A. Klein, Dr. A. Thissen, D. Kraft, F. Säuberlich, R. Fritsche and J. Fritsche in our research group for their valuable discussions and assistance, and also Prof. B. Åkermark in Stockholm University of Sweden for his friendly support. Finally, we thank the reviewers for their valuable and helpful suggestions on the modification of this manuscript.

References and Notes

(1) (a) O'Regan, B.; Grätzel, M. *Nature* **1991**, *353*, 737. (b) Nazeeruddin, M. K.; Kay, A.; Rodicio, I.; Humphry-Baker, R.; Muller, E.; Liska, P.; Vlachopoulos, N.; Grätzel, M. *J. Am. Chem. Soc.* **1993**, *115*, 6382. (c) Hagfeldt, A.; Grätzel, M. *Acc. Chem. Res.* **2000**, *33*, 269.

(2) (a) Nazeeruddin, M. K.; Humphry-Baker, R.; Grätzel, M.; Wöhrle, D.; Schnurpfeil, G.; Schneider, G.; Hirth, A.; Trombach, N. *J. Porphyrins Phthalocyanines* **1999**, *3*, 230. (b) Fang, J.; Wu, J.; Lu, X.; Shen, Y.; Lu, Z. *Chem. Phys. Lett.* **1997**, *270*, 145. (c) Yanagi, H.; Chen, S.; Lee, P. A.; Nebesny, K. W.; Armstrong, N. R.; Fujishima, A. *J. Phys. Chem.* **1996**, *100*, 5447.

(3) (a) He, J.; Hagfeldt, A.; Lindquist, S. E.; Grennberg, H.; Korodi, F.; Sun, L.; Åkermark, B. *Langmuir* **2001**, *17*, 2743. (b) Shen, Y.; Wang, L.; Lu, Z.; Wei, Y.; Zhou, Q.; Mao, H.; Xu, H. *Thin Solid Films* **1995**, *257*, 144.

(4) Huang, S. Y.; Schlichthörl, G.; Nozik, A. J.; Grätzel, M.; Frank, A. *J. Phys. Chem. B* **1997**, *101*, 2576.

(5) Gerischer, H.; Willig, F. *Top. Curr. Chem.* **1976**, *61*, 31.

(6) (a) Pope, M. *J. Chem. Phys.* **1962**, *36*, 2810. (b) Fan, F.-R.; Faulkner, L. R. *J. Chem. Phys.* **1978**, *69*, 3334.

(7) Rensmo, H.; Westermark, K.; Södergren, S.; Kohle, O.; Persson, P.; Lunell, S.; Siegbahn. H. *J. Chem. Phys*. **1999**, *111*, 2744.

(8) Lenzmann, F.; Krueger, J.; Burnside, S.; Brooks, K.; Grätzel, M.; Gal, D.; Rühle, S.; Cahen, D. *J. Phys. Chem. B.* **2001**, *105*, 6347.

(9) (a) Klein, A.; Loher, T.; Tomm, Y.; Pettenkofer, C.; Jaegermann, W. *Appl. Phys. Lett.* **1997**, *70*, 1299. (b) Schlaf, R.; Lang, O.; Pettenkofer, C.; Jaegermann, W.; Armstrong, N. R. *J. Vac. Sci. Technol*. **1997**, *A15*, 1365. (c) Lang, O.; Klein, A.; Pettenkofer, C.; Jaegermann, W.; Chevy, A. *J. Appl. Phys*. **1996**, *80*, 3817.

(10) He, J.; Benkö, G.; Korodi, F.; Polívka, T.; Lomoth, R.; Åkermark, B.; Sun, L.; Hagfeldt, A.; Sundström, V. *J. Am. Chem. Soc.* In press.

(11) Hagfeldt, A.; Grätzel, M. *Chem. Rev*. **1995**, *95*, 49.

(12) Shklover, V.; Nazeeruddin, M. K.; Zakeeruddin, S. M.; Barbe, C.; Kay, A.; Haibach, T.; Steuer, W.; Hermann, R.; Nissen, H. U.; Grätzel, M. *Chem. Mater*. **1997**, *9*, 430.

(13) Wagner, C. D., Riggs, W. M., Davis, L. E., Moulder, J. F., Muilenberg, G. E., Ed. *Handbook of X-ray Photoelectron Spectroscopy*; Perkin-Elmer: Eden Prairie, 1979.

(14) Rao, C. N. R.; Sarma, D. D.; Vasudevan, S.; Hegde, M. S. *Proc. R. Soc. London* **1979**, *A367*, 239−252.

(15) Sanjinés, R.; Tang, H.; Berger, H.; Gozzo, F.; Margaritondo, G.; Lévy, F. *J. Appl. Phys*. **1994**, *75*, 2945.

(16) Göpel, W.; Anderson, J. A.; Frankel, D.; Jaehnig, M.; Philips, K.; Schäfer, J. A.; Rocker, G. *Surf. Sci*. **1984**, *139*, 333.

(17) (a) See, A. K.; Thayer, M.; Bartynski, R. A. *Phys. Rev. B.* **1993**, *47*, 13722. (b) See, A. K.; Bartynski, R. A. *J. Vac. Sci. Technol. A* **1992**, *10*, 2591.

(18) Moser, J.; Punichihewa, S.; Infelta, P. P.; Grätzel, M. *Langmuir* **1991**, *7*, 3012.

(19) Redmond, G.; Fitzmaurice, D.; Grätzel, M. *J. Phys. Chem*. **1993**, *97*, 6951.

(20) Kavan, L.; Grätzel, M.; Gilbert, S. E.; Klemenz, C.; Scheel, H. J. *J. Am. Chem. Soc*. **1996**, *118*, 6716.

(21) Cahen, D.; Hodes, G.; Grätzel, M.; Guillemoles, J. F.; Riess, I. *J. Phys. Chem. B* **2000**, *104*, 2053.

(22) Bard, A. J. *J. Phys. Chem*. **1982**, *86*, 172.

(23) (a) Onishi, H.; Egawa, C.; Aruga, T.; Iwasawa, Y. *Surf. Sci*. **1987**, *191*, 479. (b) Clark, D. T.; Kilcast, D.; Musgrave, W. K. R. *J. Chem. Soc. Chem. Commun*. **1971**, 517. (c) Grunze, M.; Lamb, R. N. *Chem. Phys. Lett*. **1987**, *133*, 283.

(24) (a) Gervais, M.; Douy, A.; Gallot, B.; Erre, R. *Polymer* **1986**, *27*, 1513. (b) Meyer, H. M.; Anderson, S. G.; Atanasoska, L. *J. Vac. Sci. Technol*. **1988**, *A6*, 30.